Is the Alexander-Orbach Conjecture Suitable for Treating Diffusion in Correlated Percolation Clusters?

Ommar Cruz, Ricardo Hidalgo, Salomón Alas, Salomón Cordero, Laura Meraz, Raúl Lopez and Armando Dominguez

Reprinted from

Adsorption Science & Technology

2011 Volume 29 Number 7

Multi-Science Publishing Co. Ltd.
5 Wates Way, Brentwood, Essex CM15 9TB, United Kingdom

Is the Alexander–Orbach Conjecture Suitable for Treating Diffusion in Correlated Percolation Clusters?†

Ommar Cruz[1], Ricardo Hidalgo[1], Salomón Alas[2], Salomón Cordero[1], Laura Meraz[3], Raúl Lopez[4] and Armando Dominguez[1*] *(1) Departmento de Química, UAM–Iztapalapa, P.O. Box 55-534, México D.F., México. (2) Departmento de Ciencias Naturales, UAM–Cuajimalpa, C.P. 01120, México D.F., México. (3) Departmento de Biociencias e Ingeniería, CIIEMAD-IPN, Calle 30 de Junio de 1520 S/N, Col. Barrio la Laguna Ticomán, Delg. Gustavo A. Madero. C.P. 07340, México D.F., México. (4) Departmento de Física, Instituto de Física Aplicada, Universidad Nacional de San Luis–CONICET, Av. Ej. de los Andes 950(5700), San Luis, Argentina.*

(Received 2 May 2011; accepted 16 July 2011)

ABSTRACT: How does a particle diffuse inside a percolation cluster? This question is of both scientific and practical importance, e.g. in drug-controlled release and vapour adsorption. Diffusion in fractal media is characterized by the fracton dimension, d_s. The Alexander and Orbach conjecture indicates that $d_s = 4/3$ for diffusion in classical percolation clusters and, after much research on the subject, it is still provides a very good approximation for d_s in the case of uncorrelated percolation cluster structures. However, what happens to the value of d_s when a particle is moving inside a correlated percolation cluster? In this work, this problem is studied via Monte Carlo computer simulation. Our results show that the Alexander and Orbach conjecture is not always fulfilled.

1. INTRODUCTION

Alexander and Orbach have suggested that the fracton dimension of infinite percolation clusters is $d_s = 4/3$, this value being for all dimensions (i.e. 2D, 3D, etc.) larger than one (Alexander and Orbach 1982; Kozma and Nachmias 2009). To date, there have been numerous attempts to prove or refute this notable result; nevertheless, this conjecture has shown to be a good approximation for particle diffusion in random heterogeneous media (Ben-Avraham and Havlin 2004). A particle moving via diffusion through a porous medium is an important topic in many domains, e.g. in medication by controlled drug release (Villalobos *et al*. 2006) and in vapour sorption kinetics in solid porous media (Watt-Smith *et al*. 2006), amongst others. The mathematical modelling of mass transport within porous media has generally been made by using network models [or graphs, as mathematicians term them (Burioni and Cassi 2005)] to represent the morphology of the void space. These graphs allow much of the structural intricacy of the void space to be included in the model, while still retaining an adequate mathematical tractability (Mayagoitia 1993). In these models, pore sizes are sampled from a measured probability density function and are randomly assigned to lattice elements. However, spatial correlation and directionality are frequently observed in real porous media (Vidales *et al*. 1996; Domínguez *et al*. 2000), and there is evidence that these variables exert significant effects on the shape and kinetics of phenomena occurring

† Published in the Festschrift of the journal dedicated to Professor Giorgio Zgrablich on the occasion of his 70th birthday and to celebrate his 50 years as a faculty member at the National University of San Luis in Argentina.

* Author to whom all correspondence should be addressed. E-mail: doar@xanum.uam.mx.

inside these media (López *et al*. 2007; Felipe *et al*. 2005). For instance, the fractal dimension of a sample-spanning invasion percolation cluster is a non-universal amount and varies with the spatial correlation (López *et al*. 2003).

Almost all systems can be represented as networks in which the elements of the system can form nodes, with these nodes being considered as linked together only if interactions exist between them. The advantage of viewing systems as networks is that much of their thermodynamic behaviour is determined by the pattern or topology of the network linkage, rather than what passes across the links. Initially, this appeared a surprising idea, but recent research has shown it to be true (Burioni and Cassi 2005). Thus, one can infer a great deal about how a system will behave by observing its network topology, i.e. the precise sequence, statistically expressed, in which the numerical labels of the network elements are distributed throughout the graph. In fact, either within a homogeneous medium (i.e. that depicting a very large correlation) or within a random heterogeneous medium (i.e. no correlation), there is a range of different situations. It has now been realized that the network structures of most systems observed in Nature lie midway between being more disordered than regular lattices, although more structured that random graphs (Finnigan 2005). The Dual Site–Bond Model (DSBM) provides an elegant way of modelling the structure of a complex medium (Mayagoitia 1993; Cordero *et al*. 2004). This model produces correlated networks characterized by diverse degrees of correlation among the network elements.

In the present work, porous media have been modelled as infinite percolation clusters generated from correlated networks constructed via the DSBM. The percolating objects have the advantage of being relatively easy to mimic with real materials and are useful for testing our understanding regarding diffusion on fractal and disordered materials. As mentioned earlier, the percolation cluster structure is a function of the network correlation. In order to study how the cluster configuration affects the transport properties through the porous medium, we have analyzed a simple random particle walk inside infinite percolation clusters (Bunde *et al.* 2007; Kim *et al*. 2007). The results of such a study are reported below.

2. METHOD

The research method followed throughout this work may be sub-divided into three procedures.

1. The creation of diverse numerical square lattices endowed with different degrees of spatial correlation among their constitutive entities; these lattices are constructed by means of the DSBM Monte Carlo method reported by Cordero *et al*. (2001) and characterized via a correlation length, ξ.
2. *Model of a porous medium.* Such media are generated by classical percolation clusters formed within correlated lattices and are characterized by both their lacunarity, Λ (Luo and Lin 2009) and their fractal dimension, d_f (Stanley 1996).
3. A Monte Carlo study of the diffusion occurring inside the generated porous media, and the characterization of this process by means of both the diffusion exponent, d_w, and the spectral dimension, d_s (Ben-Avraham and Havlin 2004).

2.1. DSBM: metric segregation and directionality in networks

A complex system is a system composed by interconnected parts that, as a whole, exhibits one or more properties which are not evident from the properties of the individual parts (Finnigan 2005). A porous medium fits this definition very well, although it appears at first sight to be in disorder;

nevertheless, it follows amazing morphological laws (Mayagoitia 1993). Many models have been used to represent correlations in these media and to analyze transport properties in them. Networks have been used to represent porous media and, in this context, we have notably worked with the DSBM and found interesting behaviours — cf. Cordero *et al*. (2004), for example, and references cited therein.

In order to present our points and results as straightforwardly as possible, we provide a résumé of the DSBM as follows:

- To decompose the complex system into two types of interrelated elements, "sites" and "bonds"; each plays a different role in the network that must be clearly recognized. The sites and bonds are arranged together in a particular lattice configuration, a square lattice in this case where sites are located at the nodes while each bond connection is located in between two adjacent sites, i.e. two sites are associated with each bond and four bonds are connected to each site.
- To identify a "metric", R [for example, an adsorption energy in the case of a solid surface (Mayagoitia *et al*. 1989) or a capillary energy in the case of a porous medium (Domínguez *et al*. 2001)]. To attach a metric value distribution to each type of element, i.e. one distribution for sites, and another one for bonds, each element of the system is labelled by just one value of the metric. In order to compare this property between the two kinds of elements, the nature of the metric has to be the same for both sites and bonds. Let $F_S(R_S)$ and $F_B(R_B)$ be the probability density functions associated with the site metric R_S and the bond metric R_B, in this order.
- To recognize from the very definitions of "site" and "bond", a *construction principle*, viz. an obvious and constant neighbouring relationship between the metric of each site and the metric of any of its corresponding bonds. For instance, in a porous medium, the capillary energy of a site is never larger than the capillary energy of any of its matching bonds (Cordero *et al.* 2004). The way in which sites and bonds are interconnected to form a network representing a given spatial arrangement is expressed by the joint probability density function, $F(R_S,R_B)$, of finding a site of metric R_S connected to a bond of metric R_B. This local restriction is written as:

$$F(R_S, R_B) = 0 \quad \text{if} \quad R_S < R_B \quad \text{otherwise} \quad F(R_S, R_B) > 0 \tag{1}$$

Equation (1) is the cornerstone of the DSBM. It expresses the fact that the metric of any bond cannot be bigger than that of its two connected sites. In this way, when the network is built, the metrics of sites and bonds that are set together must fulfil this equation. Now, in order to provide a clear notion of the anisotropy introduced in the network by means of equation (1), let us state the joint probability function in terms of both the bond-metric and the site-metric distribution functions, in the form:

$$F\left(R_S, R_B\right) = F_S\left(R_S\right)F_B\left(R_B\right)\Phi\left(R_S, R_B\right) \tag{2}$$

In equation (2), the correlation function $\Phi\left(R_S, R_B\right)$ encloses the information about the site–bond assignment procedure within the network. In order to examine the way by which the elements are interconnected throughout a simulated arrangement, we denote by Ω the overlapping area between the site-metric and the bond-metric distribution functions, $\Omega \in [0,1]$. It is well known that Ω determines the topology of the simulated network (Vidales *et al*. 1999; Román-Alonso *et al*. 2011). A large Ω value involves a clearer structuralization of the network and, therefore, a *metrics-segregation* effect that can be quantified by means of a correlation length, ξ. This length represents the mean extent (in lattice units) of patches where elements of similar metrics co-exist.

An empirical equation relating ξ to Ω has been established for networks built by means of the network construction method reported in López *et al*. (2000):

$$\xi = \frac{2\Omega^2}{\left(1 - \Omega\right)^2} \tag{3}$$

The co-domain of this continuous function is the set $[0,\infty]$; $\xi = 0$ if $\Omega = 0$, and $\xi \to \infty$ if $\Omega \to 1$. The network elements are not correlated at all if $\xi = 0$, i.e. their associated labels are distributed at random throughout the network; while $\xi \to \infty$ signifies that a label segregation takes place in such a way that the network is structured into a collection of homogeneous regions of different labels; however, in each homogeneous region, sites and bonds have virtually the same numeric label. In brief, the DSBM scheme based on Ω renders simulated media of different topological configurations.

Note that equation (3) is strictly valid for square networks prepared as described in López *et al*. (2000). However, for the construction method employed in this work (Cordero *et al*. 2001)], no relationship has been established between ξ and Ω. For this reason, to explore the way by which graph elements are interlinked inside a simulated site–bond lattice, a correlation length is calculated employing the method advanced by Villalobos *et al*. (2006) and Román-Alonso *et al*. (2011). A suitable means by which the correlation length may be calculated is via the equation:

$$C(r) = \exp\left(-\frac{r}{\xi}\right) \tag{4}$$

where C(r) is the correlation coefficient existing between the metrics of any two sites of the network that are separated by a distance r, and ξ is the typical correlation length of the network. The correlation coefficient, C(r), can be calculated from:

$$C(r) = \frac{\left\langle \left(R_{S_i} - \overline{R_S}\right)\left(R_S(r) - \overline{R_S}\right)\right\rangle}{\left\langle \left(R_S(r) - \overline{R_S}\right)^2\right\rangle} \tag{5}$$

where R_{S_i} is the numerical label of site i. The mean label values cover all the sites that constitute the simulated lattice. The quantity $\overline{R_S}$ is the mean metrics value of sites in the simulated network, while $R_S(r)$ is the mean metrics value of sites separated by the distance r from site i.

The problem of the numerical generation of DSBM networks has been carefully investigated by, for example, Cordero *et al*. (2004) and Román-Alonso *et al*. (2011). Different methods have been proposed for developing networks for diverse topological properties. In this work, we report results obtained from the method employed for generating porous networks (Cordero *et al*. 2001) which enabled square networks having 500 sites per edge to be built. The resulting network is a numerical (real figures) matrix, whose entries represent the value of the metrics employed to recognize the constitutive elements. The metrics of bonds and sites are chosen from pre-arranged log-normal population samples. Eleven overlap values have been used, $\Omega \in \{0.02, 0.15, 0.23, 0.34, 0.47, 0.52, 0.63, 0.70, 0.76, 0.81, 0.86\}$, and 100 networks have been built for each Ω value. As a consequence, each quantity presented as a function of Ω in Section 3 below is an average over 100 realizations. The error of the measured quantity is equal to the standard deviation of the realizations set.

2.2. Classical percolation model of the porous medium

Spanning classical-percolation clusters have been used as models of porous media in the present work. These were constructed within the networks described above by means of a classical percolation procedure (Bunde and Havlin 1996). Conversion of the network constituted by real values into a binary format was performed via the selection of a threshold figure. In this way, a binary set-up with permeable and impermeable zones was achieved. For each network, the critical site-percolation threshold was determined as follows:

- A threshold value rendering a permeable fraction $\rho_c \approx 0.593$ was chosen by means of a trial-and-error routine. This value of ρ_c is the square lattice site-percolation threshold reported in the literature which is strictly true for random arrangements.
- Next, a set of threshold values was taken in the vicinity of that corresponding to ρ_c.
- Following the application of each threshold on the resulting binary arrangement, the existence of an infinite percolation cluster was determined by using the cluster-labelling method offered by employing the Mathematica Version 8 commands for general image and data processing. This program allows the identification of each one of the clusters contained in the binary system, cf. Figure 2 below. All the lateral boundaries of the network are assumed to be closed to any type of fluid flow, with the exception of two *producing sites* which are located at opposite edges of the lattice.
- The critical percolation threshold is the infimum value of the set of threshold values that can produce an infinite cluster from the two producing sites of the binary network. A porous medium is represented by the spanning cluster corresponding to this critical threshold. In our case, this infinite cluster represented the porous medium in which the diffusion of one particle was studied as described in Section 2.3 below.

The spanning cluster structure is characterized by both Λ (Luo and Lin 2009) and d_f (Stanley 1996). Lacunarity is strongly related to the size distribution and spatial re-partition of the holes existing in the cluster structure; roughly speaking, it quantifies the deviation from translational invariance. The more lacunar a cluster is, the more heterogeneous is the spatial arrangement of its holes, which then become large. The quantity Λ is then a measure of how data can fill the space. In this work, we have used ImageJ software[1] to analyze each spanning percolation cluster. The lacunarity was measured used the FracLac tool[2]. The measurement of Λ by FracLac is based on the gliding box method for binary data (Allain and Cloitre 1991). Further information related to the cluster Λ structure can be obtained from the estimation of d_f, which quantifies the degree of irregularity or fragmentation of an object with a spatial pattern. The commonest procedure to quantify the fractality of a binary image is via the box-counting method (Rothschild 1998) which provides the fractal dimension of the infinite cluster. By definition, ideal fractals have an infinitely fine structure and a spatially infinite extension. When such a fractal is used to model a real physical system, it is necessary to introduce two cut-off lengths: a lower cut-off length given, for example, by the lattice constant, and an upper cut-off length due to the finite size of the system considered. For a self-similar object at the length scales between these two cut-off lengths, the fractal framework is a satisfactory model for a disordered system while the box-counting method provides a very adequate method for measuring d_f (Theiler 1990).

[1] http://rsbweb.nih.gov/ij/;.http://rsb.info.nih.gov/ij/. [2] http://rsbweb.nih.gov/ij/plugins/fraclac/fraclac.html.

2.3. Random walk inside percolation clusters

In this work, the diffusion process is modelled by a simple random walk (Havlin and Bunde 1996; Metzler and Klafter 2000), by which the particle moves one step of length equal to the lattice unit each time unit; the final site to which the particles arrives is randomly chosen among the nearest-neighbour sites in the given lattice. Note that a time unit corresponds to one Monte Carlo step. Monte Carlo simulations of the diffusion of one particle in a porous medium were carried out in the percolation clusters mentioned earlier. The goal was to study the consequences of the spatial correlation existing among the pore entities with respect to mass transfer occurring by diffusion. The diffusion process can be characterized by considering the development of the mean-square displacement $\left\langle r^2(t)\right\rangle$, where r is the distance travelled from the starting point by the random walker in the time t. When diffusion takes place in an ordered medium, e.g. a crystalline material, a linear relationship arises between the mean-square displacement and the time. This is referred to as regular or *normal diffusion*. Nonetheless, several systems exhibit another kind of behaviour that is called *anomalous diffusion*. Some examples based on experimental evidence of this phenomenon can be found in Klemm *et al*. (1999, 2002), and with respect to the numerical studies employed here see Smith *et al*. (1999), Murase *et al*. (2004) and Nicolau Jr. *et al*. (2007). In terms of d_w, anomalous diffusion may be expressed as:

$$\left\langle r^2 \right\rangle \propto t^{2/d_w} \tag{6}$$

Note that $d_w = 2$ corresponds to normal diffusion, while $d_w > 2$ implies sub-diffusive behaviour in which the walker progresses more slowly than in normal diffusion. This anomaly is due to the disordered structure of the substrate in which diffusion is constrained to take place. For example, in 2D percolation clusters, we note the presence of dead ends (or dangling ends) — these are parts of the structure where the walker is forced to return over a previous path. Hence, in this problem, it is paramount to relate the structural properties of the medium with the diffusion properties. Traditionally, d_f, d_w and d_s are related by the following equation:

$$d_s = 2d_f/d_w \tag{7}$$

where the fracton dimension, d_s, characterizes the time evolution of the number of distinct sites that are visited by a random walker, S(t), such that:

$$S(t) \propto t^{d_s/2} \tag{8}$$

The Alexander and Orbach conjecture suggests the existence of a “super-universal” fracton dimension, i.e. $d_s = 4/3$ for diffusion in self-similar fractal media such as percolation clusters (Ben-Avraham and Havlin 2004; Zabolitzky 1984).

For each *in situ* experiment, simulation of a random walk occurring inside a spanning cluster, d_w, is computed via equation (6). Each dimensional value computed here corresponds to an average of over 100 realizations, and its absolute error is equal to the standard deviation of the realization set. Also, the values of S(t) are computed as an average over 100 realizations. The reported d_s values are calculated via both equations (7) and (8). The incumbent values are presented and discussed in Section 3 below.

3. RESULTS

3.1. Correlated graphs

It is pertinent to point out that the network size effect is not considered as a variable here. The network size used in this work, viz. 500 × 500 sites, was large enough to guarantee no border effects and good statistical representation (Bunde and Havlin 2004). The largest ξ value used in this study was ca. 12 lattice units, as may be observed in Figure 1. Hence, all the ξ values computed in this work were very small relative to the extent of the chosen network. Figure 1 shows ξ values for $\Omega \in [0.40, 0.87]$; $\xi \approx 0$ for $\Omega < 0.42$. Note that ξ varies strongly in going from the least to the most correlated networks. For example, in networks built with $\Omega = 0.01$, ξ is virtually zero; this means that significant large regions where elements of similar labels can co-exist are almost absent in this arrangement. However, the situation is radically different as overlap increases. When $\Omega = 0.86$, $\xi \approx 12$, which means that, in this case, patches spread over a region which is ca. 12 sites long and wide. The best data fit leads to an exponential relationship, viz.:

$$\xi = 0.78 \exp\left(6.60\,\Omega^{5.79}\right) \tag{9}$$

This behaviour is qualitatively akin to that obtained by other network construction methods based on the DSBM (Cordero *et al*. 2004), i.e. a negligible influence of Ω on the network structure occurs when $\Omega \leq 0.5$, while a strong effect arises when $\Omega > 0.5$. However, in quantitative terms, these methods exhibit a non-common behaviour as can be detected by contrasting equations (3) and (9). Thus, we consider that the network construction method employed in the present work is comparable to other Monte Carlo approaches as presented by Cordero *et al*. (2001), in that it provides numerical square networks characterized with different topologies ranging from $\xi = 0$ to $\xi \approx 12$. Given the size of the networks used in this study, i.e. 500 × 500, this ξ range is adequate for studying the consequences of network topology on both the spanning cluster structure and the diffusion problem.

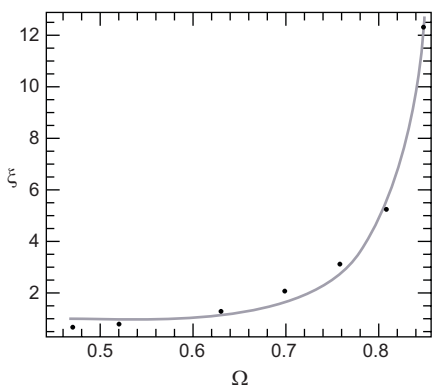

Figure 1. Plot of the correlation length, ξ, (site-to-site) versus Ω. Numerical simulation results and best data fit: $\xi = 0.78 \exp\left(6.60\,\Omega^{5.79}\right)$; for $\Omega < 0.42$, $\xi \approx 0$. The relative data error is bounded by 0.03.

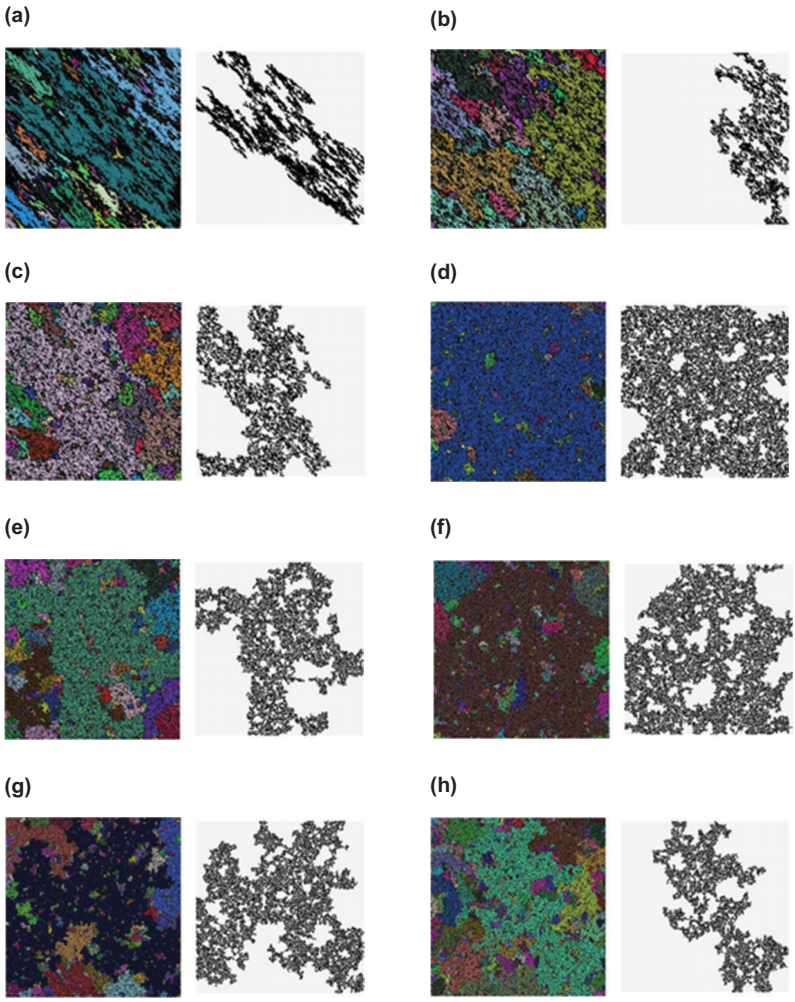

Figure 2. Porous medium = infinite percolation cluster in 500 × 500 site networks; the permeable fraction is depicted in black while the impermeable fraction is in white. The network boundaries are closed to any type of fluid flow with the sole exception of two producing sites located at opposite edges of the lattice. The figure provides an illustration of both clusters labelling and infinite clusters for some Ω and ξ values. The values corresponding to each image are: (a) Ω = 0.86, ξ = 12.29; (b) Ω = 0.81, ξ = 5.22; (c) Ω = 0.70, ξ = 2.09; (c) Ω = 0.70, ξ = 2.09; (d) Ω = 0.52, ξ = 0.80; (e) Ω = 0.47, ξ = 0.66; (f) Ω = 0.34, ξ ≈ 0; (g) Ω = 0.23, ξ ≈ 0; (h) Ω = 0.15, ξ ≈ 0.

3.2. Classical percolation clusters

Representative examples of the results regarding the influence of Ω on the patterns of classical percolation clusters are presented in Figure 2. Such visualizations show the typical characteristics of classical percolation clusters (Bunde and Havlin 1996; Ben-Avraham and Havlin 2004), i.e. the irregular shapes of the permeable phase together with some trapping of the impermeable phase. The main point arising from Figure 2 is that the DSBM scheme based on Ω is very capable of creating a wide variety of topologies, as is evident from the images shown by

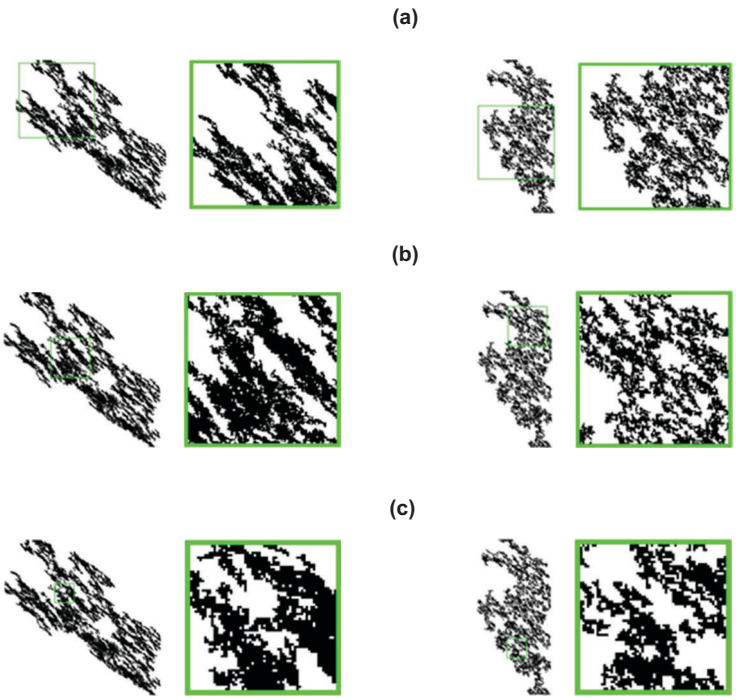

Figure 3. Self-similarity of percolation clusters in correlated networks endowed with isotropic dilatation symmetry, demonstrating the dilatation invariance of the spanning clusters presented in Figure 2. In terms of the number of sites, the sizes of the images are: (a) 250 × 250; (b) 125 × 125; and (c) 62 × 62. The size of the original window is 500 × 500 sites.

the resulting spanning clusters. Note that the shape of the infinite cluster (porous medium) goes from an isotropic structure to an anisotropic one as Ω increases. A very clear anisotropy is observed if $\Omega \geq 0.7$. Hence, the structure of the spanning cluster arises from two effects. In the network construction method employed here, the increase in Ω involves two additive effects: strong metrics segregation and some directionality. The spanning cluster becomes dense as Ω increases due to metrics segregation; consequently, the detail of the cluster structure diminishes as Ω increases. On the other hand, directionality promotes preferential trails; the spanning cluster becomes narrower (it tends to be more linear as $\Omega \rightarrow 1$) and fills the space more poorly as Ω increases. Directionality is the main source of cluster anisotropy. Figure 3 illustrates that, despite the anisotropy exhibited by some of the spanning clusters obtained, all the infinite clusters presented in Figure 2 have self-similar structures. It should also be observed that these arrangements are endowed with isotropic dilatation symmetry. Notice that the anisotropy, as such, implies no self-affinity; self-affinity is an attribute of an object possessing anisotropic dilatation symmetry (Mandelbrot 1985).

In order to quantify the effects of network topology on the spanning cluster structure, the information about cluster complexity at different scales can also be presented in terms of parameters such as Λ and d_f. Figure 4 overleaf presents the dependence of Λ on Ω. The best fit of the data provides the following exponential relationship:

$$\Lambda = 0.18e^{1.95\Omega^{10.98}} \tag{10}$$

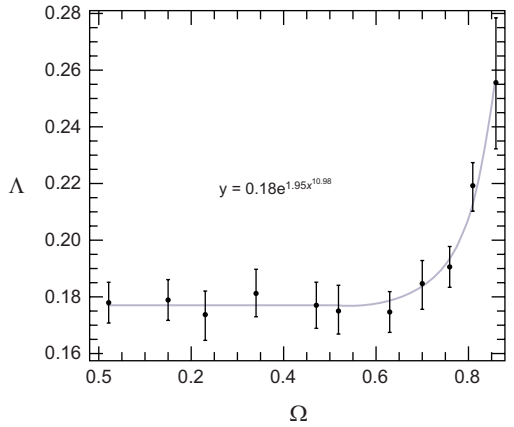

Figure 4. Plot of the lacunarity of the porous medium, Λ, versus Ω. Data obtained from network simulation and best data fit.

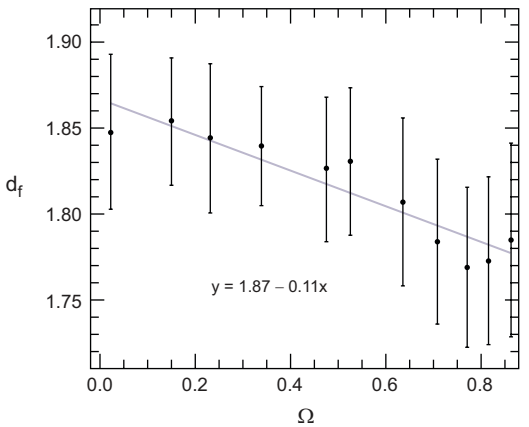

Figure 5. Plot of the fractal dimension of the porous medium, d_f, versus Ω. Data obtained from network simulation and best data fit.

In a similar manner to ξ, the behaviour of Λ follows two different trends: its value becomes small and is practically invariable for $\Omega \leq 0.5$, whilst it grows very rapidly for $\Omega > 0.5$. As a consequence, the size of the holes increases as Ω increases; this means that the cluster texture is gradually lost as Ω changes from zero to one. The information presented in Figure 5 shows the dependence of d_f on Ω and supports the previous observation that the texture of the porous medium is lost when Ω increases. Overall, the value of d_f decreases as Ω increases. The best data fit gives the following linear relationship:

$$d_f = 1.87 - 0.11\Omega \tag{11}$$

As mentioned earlier, this outcome is the result of two combined effects. The fractal dimension is an estimation of the level of detail of the spanning cluster. Densification leads to more efficient

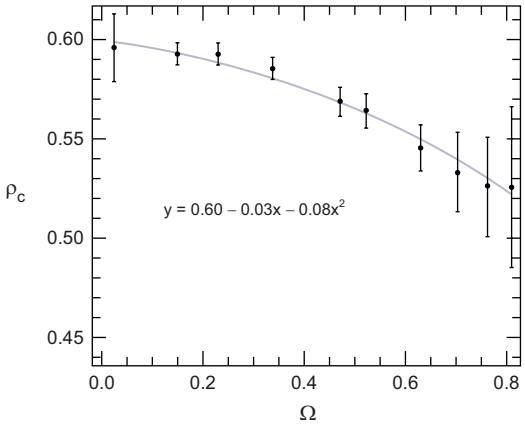

Figure 6. Classical percolation threshold. Plot of the critical site-percolation threshold for correlated square networks as a function of Ω. Data obtained from network simulation and best data fit.

space filling; however, under these circumstances, the detail of the structure is lost and then d_f diminishes. On the other hand, although of lesser significance, directionality reduces the cluster space saturation (the spanning cluster becomes more linear as $\Omega \rightarrow 1$); under these circumstances, d_f decreases as Ω increases. In general, we observe that the network topology affects the classical percolation properties of the medium. For example, the critical percolation threshold, ρ_c, is also a function of the graph correlation. Figure 6 shows the behaviour of this value as a function of Ω. Each critical threshold presented here corresponds to an average over 100 realizations. Note that the critical threshold value changes from 0.6 (very near to 0.598, the critical threshold reported in the literature for uncorrelated networks) for $\Omega = 0.15$ to 0.53 for $\Omega = 0.81$, i.e. the critical threshold decreases as Ω increases due to the rising spanning cluster directionality.

The very similar behaviour presented by the correlation length of the network as well as by the lacunarity of the percolation cluster should be highlighted. These variables provide a better route for characterizing the static properties of the system under consideration than the cluster fractal dimension which is less sensitive to the structuralization of the network.

3.3. Diffusion in porous media

Diffusion in percolation clusters is fundamentally different from that found in regular spaces (Bunde *et al*. 2007). The difference is due to the disorder found in the heterogeneous substrates in which such transport is constrained to occur. In dealing with this problem, it is paramount to relate the structural properties of the medium to the diffusion properties. In fractal bodies, diffusion becomes anomalous, i.e. $d_w > 2$, thus implying sub-diffusive behaviour. The value of d_w increases as transport by diffusion becomes more difficult. Since the trajectory of the random walk is limited by the texture of the porous medium, it should also be noted that the behaviour of d_w as a function of Ω is closely related to the behaviours observed for Λ and ξ. For $\Omega \leq 0.5$, d_w is a constant value, but when $\Omega > 0.5$ a sharp decrease is noted in this quantity. Figure 7 overleaf shows such behaviour. The best data fit gives:

$$d_w = 2.73e^{-0.45\Omega^{6.44}} \tag{12}$$

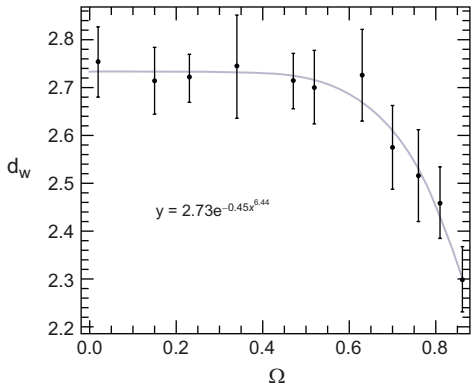

Figure 7. Plot of the diffusion dimension d_w versus Ω. Data obtained from Monte Carlo simulation and best data fit.

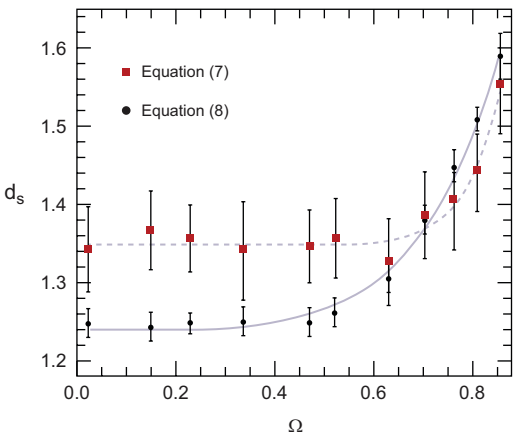

Figure 8. Plot of the fracton dimension d_s versus Ω. Data obtained from Monte Carlo simulation and best data fit. The data points depicted correspond to the following: (■) d_s calculated via equation (7); (●) d_s calculated via equation (8).

The diffusion process in fractal media can be characterized by means of the spectral dimension, d_s. Figure 8 shows the observed dependence of d_s on Ω resulting from our simulations associated with data arising from equations (7) and (8). It should be noted that the behaviour of d_s is very similar to those observed for ξ and Λ. The data set arising from equation (8) fulfils the Alexander–Orbach conjecture, i.e. $d_s \approx 4/3$ when $\Omega \leq 0.5$. When $\Omega > 0.5$, $d_s > 4/3$, thereby suggesting a more efficient mass diffusion than that stated by the Alexander–Orbach conjecture. The magnitude of d_s increases as Ω increases, while a significant deviation from the conjecture is observed when $\Omega \rightarrow 1$. A theoretical explanation of this result has yet to be found. The metrics segregation produces permeable zones which are free from impermeable obstacles. The size of these zones increases as the porous media correlation increases. From a typical value of $d_s = 4/3$ for a classical percolation cluster built for random media, the increase in d_s follows an exponential relationship represented by:

$$d_s = 1.24e^{0.51\Omega^{4.62}} \quad (13)$$

In brief, spatial correlation can improve mass transfer by diffusion in porous media; the reduction of detail in the cluster texture improves the mass transit.

It should be noted that the data set arising from equation (8) presents a small but persistent gap from $d_s = 4/3$ when $\Omega \leq 0.5$. At present, we are unable to advance any explanation for this behaviour. When $\Omega > 0.5$, the data sets depicted in Figure 8 behave in a very similar fashion. Under these circumstances, equation (7) is still valid for diffusion in correlated percolation clusters.

4. CONCLUSIONS

The main conclusions arising from the work described are as follows:

- The DSBM is a simple approach capable of describing complex media with different topological structures. These are generated by varying a single parameter, Ω, viz. the overlap between the site- and the bond-metrics distribution functions. The quantity Ω can be associated with a correlation length, ξ, in such a way that $\xi \to 0$ as $\Omega \to 0$ and $\xi \to \infty$ as $\Omega \to 1$. From this concept, it has been possible to create porous structures with different topological properties.
- In general, we have found that the percolation properties of the medium change with the correlation existing among the network elements, e.g. the critical percolation threshold is a function of Ω.
- From the diffusion simulation results, it has been found that the value of the spectral dimension, d_s, is a function of the topology of the porous medium. Significant deviation from the Alexander and Orbach conjecture, viz. $d_s = 4/3$, was observed when the porous medium elements adopted a clear spatial correlation. Other evidence advanced against the Alexander and Orbach conjecture has been cited by Zabolitzky (1984).
- A very clear relationship has been found among the following variables: fracton dimension, lacunarity of the porous media and the length of the network correlation.

ACKNOWLEDGEMENTS

Thanks are given to CONACYT for the support provided under Project No. 83659 “Estudio Fisicoquímico de la obtención y de las propiedades de los sólidos mesoporosos”. Thanks are also due to the SEP-PROMEP Network “Fisicoquímica de Sistemas Complejos Nanoestructurados” and Project “Estudio de Propiedades Fisicoquímicas de Sistemas Complejos Nanoestructurados (UAM-I-CA-31 Fisicoquímica de Superficies)”. Dr. S.J. Alas would like to thank PROMEP-SEP for financial support through Project No. 47310210.

REFERENCES

Alexander, S. and Orbach, R. (1982) *J. Phys. Lett., Paris* **43,** L625.

Allain, C. and Cloitre, M. (1991) *Phys. Rev. A* **44,** 3552.

Ben-Avraham, D. and Havlin, S. (2004) *Diffusion and Reactions in Fractals and Disordered Systems*, Cambridge University Press, Cambridge, U.K., Chap. 6.

Bunde, A. and Havlin, S. (Eds) (1996) *Fractals and Disordered Systems*, 2nd Edn, Springer, New York, pp. 59–113.

Bunde, A., Heitjans P., Indris S., Kantelhardt, J.W. and Ulrich, M. (2007) *Diffusion Fundam*. **6,** 9.1.
Burioni, R. and Cassi, D. (2005) *J. Phys. A: Math. Gen.* **38,** R45.
Cordero, S., Kornhauser, I., Domínguez, A., Felipe, C., Esparza, J.M., Rojas, F., López, R.H., Vidales, A., Riccardo, J.L. and Zgrablich, G. (2004) *Part. Part. Syst. Charact.* **21,** 101.
Cordero, S., Rojas, F. and Riccardo, J.L. (2001) *Colloids Surf. A* **187/188,** 425.
Domínguez, A., Bories, S. and Prat, M. (2000) *Int. J. Multiphase Flow* **26,** 1951.
Domínguez, A., Pérez-Aguilar, H., Rojas, F. and Kornhauser, I. (2001) *Colloids Surf. A* **187/188,** 415.
Felipe, C., López, R.H., Vidales, A.M. and Domínguez, A. (2005) *Adsorption* **11,** 491.
Finnigan, J. (2005) *Aust. Sci*. 32 (June issue).
Havlin, S. and Bunde, A. (Eds) (1996) *Fractals and Disordered Systems*, 2nd Edn, Springer, New York, pp. 115–175.
Kim, J.W., Perfect, E. and Choi, H. (2007) *Water Resour. Res*. **43,** w01405.
Klemm, A., Metzler, R. and Kimmich, R. (2002) *Phys. Rev. E* **65,** 021112-1.
Klemm, A., Muller, H.P. and Kimmich, R. (1999) *Physica A* **266,** 242.
Kozma, G. and Nachmias, A. (2009) *Invent. Math*. **178,** 635.
López, R.H., Vidales, A.M. and Zgrablich, G. (2003) *Physica A* **327,** 76.
López, R.H., Vidales, A.M. and Zgrablich, G. (2000) *Langmuir* **16,** 3441.
López, R.H., Vidales, A.M., Domínguez, A. and Zgrablich, G. (2007) *Colloids Surf. A* **300,** 122.
Luo, L. and Lin, H. (2009) *Vadose Zone J*. **8,** 233.
Mandelbrot, B.B. (1985) *Physica Scripta* **32,** 257.
Mayagoitia, V. (1993) *Catal. Lett.* **22,** 93.
Mayagoitia, V., Rojas, F., Pereyra, V.D. and Zgrablich, G. (1989) *Surf. Sci.* **221,** 394.
Metzler, R. and Klafter, J. (2000) *Phys. Rep.* **339,** 1.
Murase, K., Fujiwara, T., Umemura, Y., Suzuki, K., Iino, R., Yamashita, H., Saito, M., Murakoshi, H., Ritchie, K. and Kusumi, A. (2004) *Biophys. J.* **86,** 4075.
Nicolau Jr., D.V., Hancock, J.F. and Burrage, K. (2007) *Biophys. J.* **92,** 1975.
Román-Alonso, G., Rojas-González, F., Aguilar-Cornejo, M., Cordero-Sánchez, S. and Castro-García, M.A. (2011) *Microporous Mesoporous Mater.* **137,** 18.
Rothschild, W.G. (1998) *Fractals in Chemistry*, John Wiley & Sons, Inc., New York, Chap. 8.
Smith, P.R., Morrison, I.E., Wilson, K.M., Fernández, N. and Cherry, R.J. (1999) *Biophys. J.* **76,** 3331.
Stanley, H.E. (1996) "Fractals and Multifractals: The Interplay of Physics and Geometry", in *Fractals and Disordered Systems*, Bunde, A., Havlin, S. (Eds), 2nd Edn, Springer, New York, pp. 1–58.
Theiler, J. (1990) *J. Opt. Soc. Am. A* **7,** 1055.
Vidales, A.M., Miranda, E., Nazzarro, M., Mayagoitia, V., Rojas, F. and Zgrablich, G. (1996) *Eur. Phys. Lett.* **36,** 259.
Vidales, A.M., López, R.H. and Zgrablich, G. (1999) *Langmuir* **15,** 5703.
Villalobos, R., Cordero, S., Vidales, A.M. and Domínguez, A. (2006) *Physica A* **367,** 305.
Watt-Smith, M.J., Kolaczkowski, S.T., Rigby, S.P. and Chudek, J.A. (2006) *AIChE J*. **52,** 3289.
Zabolitzky, J.G. (1984) *Phys. Rev. B* **30,** 4077.